Galectin-1 binds GRP78 to promote the proliferation and metastasis of gastric cancer

QI ZHANG[1], MUHAMMAD ALI[1], YANG WANG[1], QIAN-NAN SUN[1-4], XIAO-DONG ZHU[1], DONG TANG[1-4], WEI WANG[1-4], CANG-YUAN ZHANG[1-4], HAI-HUA ZHOU[1] and DAO-RONG WANG[1-4]

[1]Department of General Surgery, Northern Jiangsu People's Hospital, Clinical Medical College, Yangzhou University; [2]Department of General Surgery, Northern Jiangsu People's Hospital; [3]General Surgery Institute of Yangzhou, Yangzhou University; [4]Yangzhou Key Laboratory of Basic and Clinical Transformation of Digestive and Metabolic Diseases, Yangzhou, Jiangsu 225001, P.R. China

Received June 9, 2022; Accepted September 9, 2022

DOI: 10.3892/ijo.2022.5431

Abstract. The present study aimed to investigate the potential molecular mechanisms by which galectin-1 (Gal-1) and glucose-regulated protein 78 (GRP78) influence the development of malignant gastric cancer (GC). Immunohistochemistry and western blotting were used to map the expression and location of the Gal-1 gene in the 80 paraffin-embedded GC samples, 16 fresh samples and surrounding tissues. Gal-1 was overexpressed and knocked down using lentiviral vectors in the human GC cell lines HGC-27 and AGS. Through the use of the Cell Counting Kit-8 assay, clone formation assay, wound healing assay, invasion assay and tumor xenograft, the possible biological roles of Gal-1 were further evaluated. The downstream interacting proteins were predicted by the BioGRID database, and GRP78 was chosen for further investigation. Immunofluorescence labeling and Co-IP were used to confirm the connection. The statistical tests utilized were the two-tailed paired Student's t-test, χ^2 test, Kaplan-Meier and Cox regression analysis, and Spearman's rank correlation coefficients. In GC, Gal-1 is extensively expressed and has the potential to interact with GRP78. Poor prognosis is linked to high levels of GRP78 and Gal-1 expression in patients with GC. According to the functional study, Gal-1 knockdown prevented cells from thriving and pushed Gal-1 expression, which aided in the proliferation, migration and invasion of GC. Gal-1 overexpression additionally aided the development of subcutaneous xenograft tumors. The mechanistic investigation proved that GRP78 and Gal-1 interacted, accelerating the course of GC. Gal-1 silencing had an inhibitory effect on the proliferation of HGC-27 cells that was removed by ectopic GRP78 expression, whereas the stimulating effects of Gal-1 overexpression in AGS cells were inhibited by GRP78 knockdown. In conclusion, Gal-1 interacts with GRP78 to facilitate the advancement of GC. The Gal-1/GRP78 axis is supported by the functional data of the present study as a possible GC treatment target.

Correspondence to: Dr Dao-Rong Wang, Department of General Surgery, Northern Jiangsu People's Hospital, Clinical Medical College, Yangzhou University, 98 Nantong West Road, Yangzhou, Jiangsu 225001, P.R. China
E-mail: wdaorong666@sina.com

Key words: gastric cancer, galectin-1, glucose-regulated protein 78, progression, prognosis

Introduction

Gastric cancer (GC) is the fourth most prevalent cancer (7.8% of all reported cancer cases) and the second major cause of mortality (9.7% of all cancer-related deaths) from cancer in 2008, accounting for 95% of primary malignant gastric neoplasms (1). Although risk factors for stomach carcinogenesis have been established, such as *Helicobacter pylori* infection, natural carcinogens (e.g., nitrates), dietary pro-carcinogens, adenomatous polyps, and heritable and family hazards, primary prevention remains a challenge (2). Due to a lack of evident or distinct symptoms in the early stages, and frequently with only a few or minimum symptoms, this leads to even advanced stage III or IV disease at the time of diagnosis. Despite the fact that surgical resection is the first-line treatment option for GC patients, and recent breakthroughs in systemic multi-line chemotherapy or postoperative adjuvant radiation paired with surgery have been found to improve patient survival (3), GC recurrence is common following surgery. As a result, it is critical to identify useful biomarkers that mediate the formation and progression of GC in order to understand in an improved way the process of gastric carcinogenesis and create effective treatments to enhance patient outcomes.

Galectin-1 (Gal-1) is a protein family member with a preference for glycoconjugate-galactose residues (4). Gal-1 was shown to be overexpressed in a variety of malignancies, including lung cancer (5), renal cancer (6), hepatocellular carcinoma (7) and ovarian cancer (8). According to evidence, altered Gal-1 expression in cancer tissues may be crucial for tumor development, growth, proliferation, metastasis, angiogenesis, immune response and resistance to systemic chemotherapy (9). The role of Gal-1 in GC remains mainly unknown from a molecular perspective.

Endoplasmic reticulum stress (ERS) or the unfolded protein response (UPR), a cellular adaptive mechanism that happens in response to the disruption of ER homeostasis, can be brought on by a variety of physiological or pathological conditions, including nutrient deprivation, Ca^{2+} depletion, hypoxia, inflammation activation and oxidative stress (10). The ER chaperone protein known as glucose-regulated protein 78 (GRP78) is also a recognized indicator of ERS. GRP78 separates from IRE1, PERK and ATF6 during ERS to start three signaling pathways (11). UPR and GRP78 are overexpressed in the early stages of ERS, which helps cells survive by lowering the amount of protein that enters the ER, blocking protein synthesis and lessening cellular stress. But when ERS is prolonged and severe, the apoptotic marker protein C/EBP homologous protein (CHOP) is increased (12). A versatile protein called GRP78 is essential in both physiological and pathological stress (13). GRP78 was strongly activated in a number of malignancies, including breast cancer, according to numerous studies (14,15), lung cancer (16), thyroid carcinoma (17), colorectal cancer (18), hepatocellular cancer (19) and prostate cancer (20). GRP78 overexpression contributed to tumor cell survival, growth, angiogenesis, and resistance to treatment. In individuals with GC, overexpression of GRP78 is associated with increased lymph node (LN) metastases and a poor prognosis (21). Cancer cells undergo growth suppression and apoptosis when exposed to GRP78 inhibitors, such as small molecules and specific binding peptides. These results revealed that the progression of GC is mediated by GRP78. However, the role of GRP78 in GC is not entirely elucidated.

As a result, it was investigated whether GRP78 played a role in the development of the tumor that Gal-1 caused in the current study. Positive connection was discovered between GRP78 and Gal-1. GRP78 was a target of Gal-1 in GC cells, according to the Co-IP data. Given that GRP78 has been linked to the spread of various malignancies, our database was utilized to confirm that there is a strong link between the high levels of GRP78 expression in GC tissues and the TNM stage. These findings suggested that the Gal-1-GRP78 axis is a viable target for the development of GC medications.

Materials and methods

Bioinformatic analysis. 'Expression Plots' of the GEPIA database (http://gepia.cancer-pku.cn/) were used to compare the expression levels of Gal-1 in tumor and normal tissues in GC (22). Oncomine (https://www.oncomine.org/resource/login.html) was used to simultaneously collect the mRNA expression levels of Gal-1 in GC and normal tissues, and the results were as follows: Cho gastric and DErrico gastric (23). Mechanistically, the interacting proteins of Gal-1 were examined using the BioGRID database (https://thebiogrid.org/) (24).

Patients and GC specimens. Human surgical clinical specimens, including formalin-fixed paraffin-embedded human GC specimens (n=80, aging from 43 to 77 years old) and fresh surgically removed GC tissues (n=16; including 9 male and 7 female, aging from 46 to 67 years old), were collected from Northern Jiangsu People's hospital, clinical medical school, Yangzhou University (Yangzhou, China) between July 2015 and May 2017. Prior to surgery, none of the patients underwent preoperative chemotherapy. At least two qualified pathologists determined that all tissues were GC. According to the American Joint Committee on Cancer TNM staging system (AJCC-8 TNM) for gastric carcinoma, the disease stage was identified. Our hospital database and clinical records were used to gather clinicopathological data on age, sex, tumor size, TNM stage, degree of differentiation, histological grade, venous and nerve invasion (Tables I and III). The present study was approved (approval no. 2019KY-022) by The Northern Jiangsu People's Hospital, the Clinical Medical School and the Ethics Committee of Yangzhou University (Yangzhou, China). Written informed consent was obtained from all participants before the study was carried out.

Immunohistochemistry (IHC). The GC samples and xenografted tumor tissues were embedded in paraffin, sectioned into 4 m-thick pieces, and set on glass slides after being fixed in a 10% formalin solution for 24 h at room temperature. They were then rehydrated with an ethanol gradient (100-50%) after being deparaffinized with xylene. After that, the sections were heated in sodium citrate antigen retrieval solution (cat. no. C1032; Beijing Solarbio Science & Technology Co., Ltd.). The slides were then incubated with normal goat serum for 30 min at room temperature after being submerged in hydrogen peroxide (0.3%; OriGene Technologies, Inc.) to block endogenous peroxidase activity. Following that, IHC staining was performed. Anti-Gal-1 rabbit polyclonal antibody (1:200; cat. no. 11858-1-AP; ProteinTech Group, Inc.) and anti-GRP78 antibody (1:200; cat. no. ab21685; Abcam) were incubated on GC patients' sections, anti-Gal-1 rabbit polyclonal antibody (1:200; cat. no. 11858-1-AP; ProteinTech Group, Inc.) and anti-Ki-67 rabbit monoclonal antibody (1:400, 9027; Cell Signaling Technology) were incubated on xenografted tumor tissues' sections for an overnight period at 4˚C. The following day, the slides were washed, incubated at 37˚C for 30 min with HRP-conjugated goat anti-rabbit IgG (1:100; cat. no. ab288151; Abcam), and then stained with hematoxylin and 3,3'-diaminobenzidine, respectively. After that, the slides were looked at and captured on camera with an Olympus BX53 fluorescent microscope (Olympus Corporation). Based on the number of positive cells and staining intensity, the Ki-67, GRP78 and Gal-1 staining was graded. The staining intensity scores are as follows: The staining intensity scores were as follows: 0 for colorless, 1 for yellow, 2 for brown, and 3 for dark brown. According to the percentage of positive cells, the scores were as follows: 0 for 0-5%, 1 for 5-25%, 2 for 25-50%, 3 for 50-75%, and 4 for >75%. Staining intensity and the percentage of positive cell values were combined to create the final score. Cases with a score of ≥5 were considered positive expression, while those with a score of ≤4 were considered negative expression.

Cell culture. The normal gastric epithelial cells GES-1 and GC cell lines (HGC-27 and AGS) were obtained from the Cell Bank of Type Culture Collection of Chinese Academy of Sciences, Shanghai Institute of Cell Biology, Chinese Academy of Science. Cell lines were cultured in RPMI-1640 medium supplemented with 10% fetal bovine serum (both from Gibco; Thermo Fisher Scientific, Inc.) containing 100 units/ml

Table I. Associations between Gal-1 expression and clinicopathological features of 80 patients with gastric cancer.

Histopathological parameters	Total number (80)	Expression level of Gal-1		P-value
		Low	High	
Age, years				0.759
<65	33	15	18	
≥65	47	23	24	
Sex				0.408
Male	51	26	25	
Female	29	12	17	
Tumor size				0.003
<6	43	27	16	
≥6	37	11	26	
Lauren type				0.797
Intestinal type	73	35	38	
Diffuse type	7	3	4	
Depth of invasion				0.049
T1, T2	29	18	11	
T3, T4	51	20	31	
Lymphonodus metastasis				0.007
N0, N1	40	25	15	
N2, N3	40	13	27	
Distant metastasis				0.026
Negative	58	32	26	
Positive	22	6	16	
TNM stage				0.015
I-II	35	22	13	
III-IV	45	16	29	
Degree of differentiation				0.849
Highly	43	20	23	
Moderately and poorly	37	18	19	
Histological grade				0.617
I	8	4	4	
II	38	20	18	
III	34	14	20	
Venous invasion				0.866
No	45	21	24	
Yes	35	17	18	
Nerve invasion				0.463
No	35	15	20	
Yes	45	23	22	
Glucose-regulated protein 78 expression				0.008
Low	38	24	14	
High	42	14	28	

Gal-1, galectin-1.

penicillin and 100 mg/ml streptomycin (cat. no. SV30010; Hyclone; Cytiva) at 37˚C in a humidified incubator containing 5% CO_2.

Cell transfection. Lentiviral vectors (called Lv-GAL-1) that were based on the GV358 (Ubi-MCS-3FLAG-SV40-EGFP-IRES-puromycin) lentiviral vector from

Shanghai Genechem Co., Ltd., were created. The negative control was an empty vector. Using two lentiviral vector-based short hairpin (sh)RNAs, RNA interference was used to knock down Gal-1 and GRP78 (Shanghai Genechem Co., Ltd.). The following target sequences were created for Gal-1: shGal-1 forward, 5'-CACCATCGTGTGCAACAGCAA-3' and reverse, 5'-TTGCTGTTGCACACGATGGTG-3'. The non-targeting shRNA (forward, 5'-TTCTCCGAACGTGTCACGT-3' and reverse, 5'-ACGTGACACGTTCGGAGAA-3) was used as a non-target shRNA control. The following target sequences were created for GRP78: shGRP78 forward, 5'-GAGCGCATT GATACTAGAAAT-3' and reverse, 5'-ATTTCTAGTATCAAT GCGCTC-3'. The empty vector GV654 was used as the lentiviral negative control. For the purpose of producing lentiviral particles, 20 μg the aforementioned vectors were co-transfected with 15 μg pHelper 1.0 (envelope plasmid) and 10 μg pHelper 2.0 (pack-aging plasmid) in the 2nd generation transfection system into 293T cells (cat. no. GNHu17; Shanghai Institute of Cell Biology, Chinese Academy of Sciences) cultured in DMEM (Hyclone; Cytiva) with 10% FBS (Hyclone; Cytiva) at 37˚C with 5% CO_2 using Lipofectamine® 2000 (Thermo Fisher Scientific, Inc.), following the manufacturer's instructions. The packaging plasmids were co-transfected 48 h later, and the virus-containing supernatant was collected. The lentivirus was then purified by ultracentrifugation at 30,000 x g for 2 h at 4˚C. Then, the lentivirus (Lv-GAL-1, the empty vector GV358, Gal-1-shRNA, or NC-shRNA) was added and co-cultured with the target cells for 24 h at 37˚C in the presence of polybrene (5 g/ml; Shanghai GeneChem Co., Ltd.) at a multiplicity of infection of 10. This was conducted after the GC cell lines had been plated into 24-well plates with $1x10^4$ cells per well. After that, the medium was changed in preparation for another 48 h of incubation at 37˚C and 5% CO_2. Then, the stably transfected cell lines were chosen using a 25 g/ml puromycin treatment for two weeks at 37˚C. In the rescue tests, Gal-1 overexpressing AGS cells were transfected with GRP78 shRNA or NC shRNA. To establish stable transfected cell lines, 25 g/ml neomycin was then added to the media for 2 weeks. The pcDNA3.1-GRP78 and the negative control (pcDNA3.1-NC) were provided by Shanghai GenePharma Co., Ltd. pcDNA3.1-GRP78 or pcDNA3.1-NC plasmids were transfected using Lipofectamine® 2000, and the control and Gal-1 knockdown HGC-27 cells were then cultured for an additional two days before being selected using G418 reagent (Sigma-Aldrich; Merck KGaA). For the ensuing experiments, the cells were gathered.

Reverse transcription-quantitative PCR (RT-qPCR). The TRIzol® reagent (Invitrogen; Thermo Fisher Scientific, Inc.) was used to extract total RNA from the cell lysate. Using the RevertAid First Strand cDNA Synthesis kit according to the manufacturer's instructions and oligos(dT) from Thermo Fisher Scientific, Inc., the concentration of total RNA was determined spectrophotometrically and cDNA was synthesized. qPCR was carried out in accordance with the manufacturer's instructions using the SYBR Green I kit (cat. no. rk21203; ABclonal Biotech Co., Ltd.) and the StepOnePlus Real-time PCR System (Applied Biosystems; Thermo Fisher Scientific, Inc.). The primer sequences were as follows: Gal-1 forward, 5'-GCTGAA CCTGGGCAAAGACAG-3' and reverse, 5'-GTTGAGGCG GTTGGGGAACTT-3' and GAPDH forward, 5'-CCACTC CTCCACCTTTGAC-3' and reverse, 5'-ACCCTGTTGCTG TAGCCA-3'. The thermocycling conditions were as follows: Initial denaturation at 95˚C for 2 min; followed by 40 cycles at 95˚C for 5 sec and 60˚C for 30 sec. The relative mRNA levels of the target gene were determined using the $2^{-\Delta\Delta Cq}$ method, with GAPDH serving as the internal control (25).

Western blot analysis. RIPA lysis buffer (cat. no. R0020; Beijing Solarbio Science & Technology Co., Ltd.) was used to lyse cells to obtain protein samples for 30 min at 4˚C. The samples were centrifuged at 13,000 x g for 20 min at 4˚C before the supernatant was collected and the protein concentration was measured using a BCA kit (cat. no. P0012; Beyotime Institute of Biotechnology). Samples were boiled for 5 min after being mixed with a 5X loading buffer solution. Equivalent extracted amounts of protein (20 μg protein per lane) from GC tissues or whole cells were then separated with 10% SDS-PAGE gel and electro-transferred onto polyvinylidene fluoride (PVDF) membranes (Thermo Fisher Scientific, Inc.). They were blocked using 5% skimmed milk for 1 h at room temperature and then incubated overnight at 4˚C with various primary antibodies, including rabbit anti-Gal-1 (1:3,000; cat. no. ab108389), rabbit anti-GRP78 (1:3,000; cat. no. ab21685; both from Abcam), rabbit anti-GAPDH (1:5,000; cat. no. AC001) and mouse-anti GAPDH (1:5,000; cat. no. AC002; both from ABclonal Biotech Co., Ltd.); the two latter antibodies were used as internal controls. Lastly, signals were detected with an enhanced chemiluminescence substrate (cat. no. P10300; New Cell & Molecular Biotech Co., Ltd.) after incubating with secondary antibody HRP-conjugated goat anti-rabbit (1:5,000; cat. no. AP132P; MilliporeSigma) or goat anti-mouse antibodies (1:5,000; cat. no. AS003; ABclonal Biotech Co., Ltd.). The intensity of western blot bands was quantified using ImageJ (version 1.51; National Institutes of Health).

Cell Counting Kit-8 (CCK-8) and colony formation assays. A total of 1,000 cells/well were plated in a 96-well plate and cultured overnight at 37˚C. After 24 h, 10 μl CCK-8 (Beyotime Institute of Biotechnology) reagent was added to each well at 24, 48 and 72 h and incubated for 2 h. Absorbance was read at 450 nm using an automatic plate reader. Triplicates of each experiment were independently performed. Additionally, a colony formation experiment was run to assess the capacity for cell proliferation. Six-well plates were seeded with $5x10^2$ GC cells per well and incubated at 37˚C for 10 days. The colonies were stained with 0.1% crystal violet at room temperature for 10 min after being fixed with 4% paraformaldehyde at room temperature for 10 min. The number of visible colonies (consisting of >50 cells) of three replicates was counted manually after the plates dried up.

Wound healing assay. In order to create a confluent monolayer, HGC-27 and AGS cells were seeded into six-well plates and cultured in serum-free RPMI-1640 medium. At day 2, when the cells grew to 80-90% confluency as a monolayer, the monolayer was gently scratched with a 200-μl pipette tip, with the tip being perpendicular to the bottom of the plate during the operation. The recovered tissues were then rinsed three

times with PBS to remove debris after scratching. To culture the remaining cells, the medium containing 3% FBS was also changed. After the scratching, images were captured at 0, 24 and 48 h under a light microscope (magnification, x200). ImageJ program examined the wound closure (version 1.51; National Institutes of Health).

Transwell migration and invasion assays. The migration and invasion assays were performed using Transwell chamber (Corning, Inc.). For the migration assay, $1x10^4$ transfected cells per well (serum-starved for 24 h) were suspended in 200 μl of serum-free RPMI-1640 medium and plated in the upper chamber of a 24-well Boyden chamber. The lower chamber contained RPMI-1640 medium with 10% FBS. For the invasion assay, Transwell (Corning, Inc.) chambers were first coated with Matrigel (cat. no. 356234; BD Biosciences) that was diluted at 1:30 with serum-free RPMI-1640 medium at 37˚C for 30 min. Cells ($1x10^4$) suspended in 200 μl of serum-free medium were seeded in the upper chamber of a microporous (8-μm pores) Transwell insert. In the bottom of the chamber, 500 μl RPMI-1640 medium containing 10% FBS was added. After incubation for 48 h at 37˚C, the chamber was removed, the cells which had not passed through the chamber membrane were removed using a wet cotton swab, and cells that migrated or invaded through the membrane were fixed with 4% formaldehyde at room temperature for 15 min and stained with 1% crystal violet staining solutions for 5 min at room temperature and images were captured under a light microscope (magnification, x200). Cell numbers in five randomly selected fields were counted.

Xenotransplantation experiment. A total of 10 4-week-old BALB/c male nude mice (weight, 18-22 g) were purchased from GemPharmatech Co. Ltd. and raised in a pathogen-free laminar flow cabinet throughout the experiments under the following conditions: Controlled humidity (30-40%), a constant temperature of 25˚C, a 12-h light/dark cycle and free access to food and water. The ethical approval (approval no. 202111020) to perform the animal experiments was obtained from the Ethics Committee for Animal Experiments of the Yangzhou University (Yangzhou, China). The experimental protocol was performed in accordance with the Laboratory Animal Guideline for Ethical Review of Animal Welfare (26). 4-week-old male BALB/c nude mice were randomly divided into Ctrl and OE-Gal-1 groups (n=5 in both groups). Under isoflurane inhalation anesthesia (1-2%), ~$1x10^6$ AGS cells of stably transfected strains Ctrl/OE-Gal-1 resuspended in 100 μl PBS were subcutaneously into the left armpit of the mice. The health and behaviour of the mice were monitored every 2 days to determine if there were difficulties eating or drinking, unrelieved pain or distress without recovery. If the tumor reached 2,000 mm^3, the animal would be euthanized as a humane endpoint. The following formula was used to calculate the tumor volume (V) every week: $V=(Width^2 \times Length)/2$. Four weeks post-inoculation, all the mice were sacrificed by cervical dislocation under anesthesia. The method of anesthesia used for the mice was CO_2 asphyxiation (CO_2 was introduced into the chamber at a rate of 40-70% of the chamber volume per min to minimize distress). Dilated pupils were then used to verify death. Then, the tumors were removed, weighed and fixed for further histopathological analyses. Immunohistochemistry was performed on xenografted tumor tissues with anti-Gal-1 rabbit polyclonal antibody (1:200; cat. no. 11858-1-AP; ProteinTech Group, Inc.) and anti-Ki-67 rabbit monoclonal antibody (1:400, 9027; Cell Signaling Technology).

Co-immunoprecipitation (Co-IP) assays. The cell lysate was harvested from HGC-27 cells using ice-cold non-denaturing lysis buffer with the addition of proteinase inhibitor cocktail Complete Mini and phosphatase inhibitor cocktail PhosSTOP (both from Roche Diagnostics). The total protein of the lysates was measured by the BCA protein assay kit (Beyotime Institute of Biotechnology) analyzed by an Eppendorf Master Photometer.

A total of 500 μl of cell lysates with a concentration of 1 μg/μl were used for Co-IP experiments performed with the Pierce Co-IP kit according to the manufacturer's instructions (Thermo Fisher Scientific, Inc.). A total of 10 μg of the monoclonal Gal-1 antibody (1:50) or GRP78 antibody (1:50; cat. no. sc166490; Santa Cruz Biotechnology, Inc.) were briefly incubated with 50 μl AminoLink Plus Coupling Resin and covalently coupled. Moreover, 10 μg non-specific IgG was set as a control. The purified protein lysate (500 μl) was pre-cleared by incubation with 80 μl of the Control Agarose Resin slurry (Thermo Fisher Scientific, Inc.) for 30 min at 4˚C on a rotator. The antibody-conjugated agarose resin was incubated with 500 μl of the pre-cleared cell lysates and rotated overnight at 4˚C. The resin was washed, and the protein complexes bound to the antibody were eluted. Subsequent proteins were separated in a 10% SDS-PAGE gel, transferred to a PVDF membrane, and detected using Gal-1 and GRP78 MAbs.

Immunofluorescence staining. HGC-27 cells were cultured for 24 h on coverslips in 24-well plates. After that, cells were washed three times and fixed in 4% paraformaldehyde at room temperature for 10 min. The cells were permeabilized with 0.1% Triton X-100 for 15 min. After blocking with 5% bovine serum albumin (Beyotime Institute of Biotechnology) at room temperature for 60 min, the cells were incubated with the following antibodies for 60 min at 37˚C: Rabbit anti-human GRP78 (1:300; cat. no. 11587-1-AP) and mouse anti-human Gal-1 (1:100; cat. no. 60223-1-Ig; both from ProteinTech Group, Inc.). The cells were washed with PBS three times and incubated for 1 h in the dark at room temperature with the following secondary antibodies: Donkey Anti-Rabbit IgG H&L (1:200; cat. no. ab150062), Goat Anti-Mouse IgG H&L (1:200; cat. no. ab150113; both from Abcam). For the experiments in which ER stress of HGC-27 cells were activated with tunicamycin (2 μg/ml; cat. no. T8480; Beijing Solarbio Science & Technology Co., Ltd.). HGC-27 cells and tunicamycin-activated HGC-27 cells were incubated with Rabbit anti-human GRP78 (1:300; cat. no. 11587-1-AP) overnight at 4˚C and then were incubated with Donkey Anti-Rabbit IgG H&L (1:200; cat. no. ab150062) at RT for 1 h. After being washed three additional times, the cells were counterstained with DAPI (Beyotime Institute of Biotechnology) at the concentration of 5 μg/ml for 5 min. The results were examined by laser scanning confocal microscopy (Leica Microsystems GmbH).

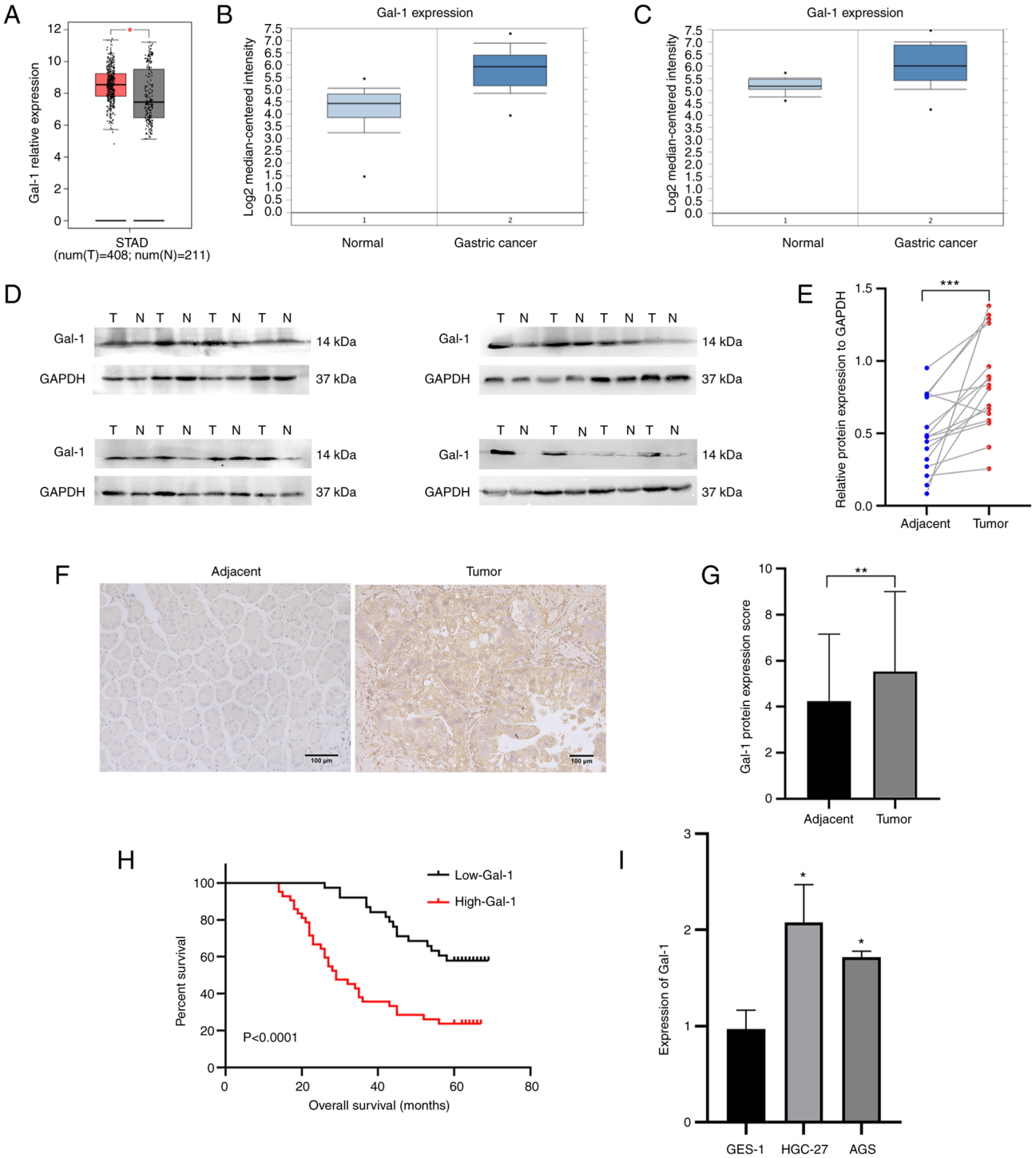

Figure 1. Gal-1 is upregulated in gastric cancer and is associated with a poor prognosis of gastric cancer. (A) Gal-1 expression in GC (n=408) and normal (n=211) samples was evaluated using the online tool GEPIA. (B and C) The box plot of expression value of Gal-1 in gastric cancer. The X-axis represents normal (left) and cancer group (right), Y-axis represents mRNA expression in log2 median/mean-centered intensity. (D) Western blot analysis results of Gal-1 in 16 pairs of normal gastric tissue and gastric cancer tissue. (E) Gal-1 expression of 16 fresh paired GC and adjacent tissue samples were determined by western blotting. (F) Immunohistochemical test results of galectin-1 in adjacent gastric tissue and gastric cancer tissue. Representative images are shown (magnification, x200). (G) Qualification of gal-1 staining in TMAs in panel F. The graph depicts the total score, the multiplication product of staining intensity and the percentage of stained cells. (H) Survival analysis of gastric cancer patients with different expression levels of galectin-1. (I) The expression level of gal-1 in normal gastric epithelial cells GES-1 and gastric cancer cells. *P<0.05, **P<0.01 and ***P<0.001. GC, gastric cancer; Gal-1, galectin-1.

Statistical analysis. At least three times each of the data were replicated. The data was examined using the statistical analysis program SPSS 24.0 (IBM Corp.). To compare two sets of independent samples, two-tailed unpaired Student's tests were utilized (Figs. 2-5). In Gal-1 and GRP78 expression in GC tissues, the data with normal distribution, and the paired 2-tailed Student's t-test was used to evaluate the significance of differences between two groups (Figs. 1E and G and 7B). One-way ANOVA and Tukey's post hoc test were used to examine measurement data between three or more groups

Table II. Prognostic factors on overall survival were analyzed by univariate and multivariate Cox's proportional hazards models in 80 patients with gastric cancer.

	Univariate analysis		Multivariate analysis	
	HR (95% CI)	P-value	HR (95% CI)	P-value
Age	0.739 (0.344-1.584)	0.437		
Sex	0.847 (0.416-1.724)	0.647		
Tumor size	2.565 (1.257-5.236)	0.010	2.350 (1.237-4.463)	0.009
Lauren type	1.854 (0.474-7.253)	0.375		
Lymphonodus metastasis	0.849 (0.308-2.339)	0.751		
Distant metastases	3.440 (1.372-8.625)	0.008	3.345 (1.682-6.648)	0.001
Depth of invasion	1.131 (0.461-2.771)	0.788		
TNM stage	4.376 (1.159-16.521)	0.029	4.014 (1.757-7.170)	0.001
Degree of differentiation	0.617 (0.289-1.314)	0.210		
Histological grade	0.961 (0.535-1.726)	0.893		
Venous invasion	0.870 (0.390-1.938)	0.733		
Nerve invasion	0.970 (0.471-1.996)	0.934		
Galectin-1	2.414 (1.033-5.641)	0.042	2.224 (1.161-4.262)	0.016
Glucose-regulated protein 78	2.614 (1.304-5.238)	0.007	2.228 (1.191-4.170)	0.012

HR, hazard ratio; CI, confidence interval.

(Figs. 1I and 6B-E). The expression of Gal-1 of GRP78 was associated with clinicopathological characteristics using a chi-squared test. The relationship between the expression of Gal-1 or GRP78 and patient prognosis was examined using the Kaplan-Meier method and log-rank test. Non-parametric Gal-1 and GRP78 expression were correlated using Spearman's rank correlation analysis. Statistics were judged significant at $P<0.05$.

Results

Gal-1 is upregulated in GC and its upregulation is associated with a poor prognosis for GC patients. The mRNA expression levels of Gal-1 were first examined in GC tissues from the GEPIA, whose RNA sequencing expression data of tumors and normal samples from TCGA public databases (http://gepia.cancer-pku.cn/) and Oncomine database in order to evaluate the significant role of Gal-1 in GC tissue. Gal-1 mRNA expression was significantly upregulated in 408 GC samples when compared with 211 instances of the normal tissues (Fig. 1A). In the two distinct validation datasets, the geometric mean of Gal-1 expression was considerably higher in GC tissues than in normal stomach samples (Fig. 1B and C). In addition, it was found that the 16 GC patients had Gal-1 protein levels. When GC tissues were compared with the nearby normal gastric tissues, it was identified that the protein level of Gal-1 was upregulated (Fig. 1D and E). IHC analysis was used to find visible Gal-1 expression levels in a developed TMA that comprised 80 matched GC and nearby normal tissues in order to understand in an improved way the role of Gal-1 in the formation of GC. When GC tissue was compared with the nearby non-cancerous tissues, Gal-1 was more highly expressed in the GC tissue (Fig. 1F and G). According to the results of the RT-qPCR investigation, Gal-1 was expressed significantly higher in GC cell lines compared with GES-1 cells (Fig. 1I). Moreover, the association between Gal-1 expression and clinicopathological characteristics was investigated, showing that higher Gal-1 expression was associated with the tumor size ($P=0.003$), depth of invasion ($P=0.049$), LN metastasis ($P=0.007$), distant metastasis ($P=0.026$), TNM stage ($P=0.015$) and GRP78 expression ($P=0.008$). However, Gal-1 expression was not associated with age ($P=0.759$), sex ($P=0.408$), Lauren type ($P=0.797$), degree of differentiation ($P=0.849$), histological grade ($P=0.617$), venous invasion ($P=0.866$) and nerve invasion ($P=0.463$) (Table I). The associations between Gal-1 expression and the overall survival (OS) of 80 patients with GC were evaluated in order to look into the connection between the expression of Gal-1 and the prognosis of GC. According to Kaplan-Meier analysis, poor OS in GC patients was positively connected with increased Gal-1 protein expression ($P<0.0001$; Fig. 1H). The factors affecting OS ($P<0.05$) were shown by univariate regression analysis to be the tumor size, distant metastases, TNM stage (stages I and II vs. stages III and IV), Gal-1 expression (low vs. high), and GRP78 expression (low vs. high). The same findings from multivariate regression analysis were obtained regarding the independent risk factors for GC progression ($P<0.05$, Table II): tumor size, distant metastases, TNM stage (stages I and II vs. stages III and IV), Gal-1 expression (low vs. high) and GRP78 expression (low vs. high). These findings suggested that Gal-1 is increased in GC and that GC patients with high levels of Gal-1 have a bad prognosis.

Gal-1 regulates proliferation, migration and invasion of gastric carcinoma. Based on the expression levels of Gal-1 in GC cell lines, Gal-1 stably overexpressing cells were

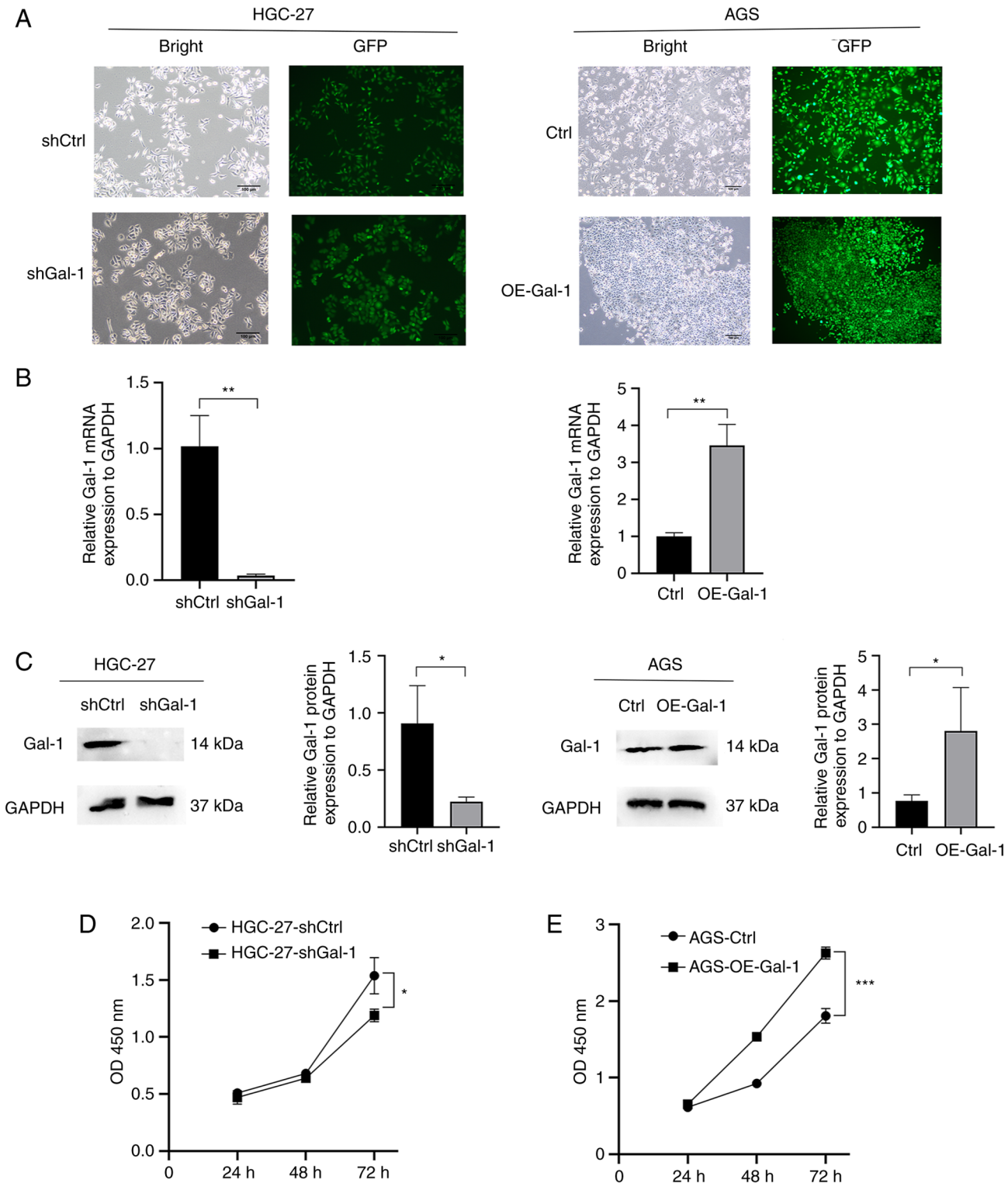

Figure 2. (A) The cell fluorescence expression was observed after 72 h-transfection (magnification, x200). (B) The knockdown efficiencies of gal-1 in the shGal-1 group in HGC-27 cells and the OE efficiencies of gal-1 in the OE-Gal-1 group in AGS cells were detected by reverse transcription-quantitative PCR. (C) Western blot analysis was used to verify the constructed galectin-1 OE and galectin-1 knockdown gastric cancer cell lines. (D and E) Detection of the proliferation of (D) HGC-27 cells after Gal-1 knockdown and (E) AGS cells after Gal-1 OE by Cell Counting Kit-8 assay. *P<0.05, **P<0.01 and ***P<0.001. Gal-1, galectin-1; sh-, short hairpin; OE, overexpression.

generated in AGS cells and the GC cell line HGC-27 was established with lentivirus-mediated Gal-1 knockdown. By using immunofluorescence analysis, RT-qPCR and western blotting, the effectiveness of Gal-1 knockdown and overexpression in HGC27 and AGS cells was verified (Fig. 2A-C). The potential of Gal-1 to influence cell proliferation was examined using the CCK-8 and colony formation assays. As revealed in Figs. 2D and 3A, cell proliferation in the shGal-1 group in HGC-27 cells was considerably lower than that in the control group (P<0.05). In addition, Transwell experiments

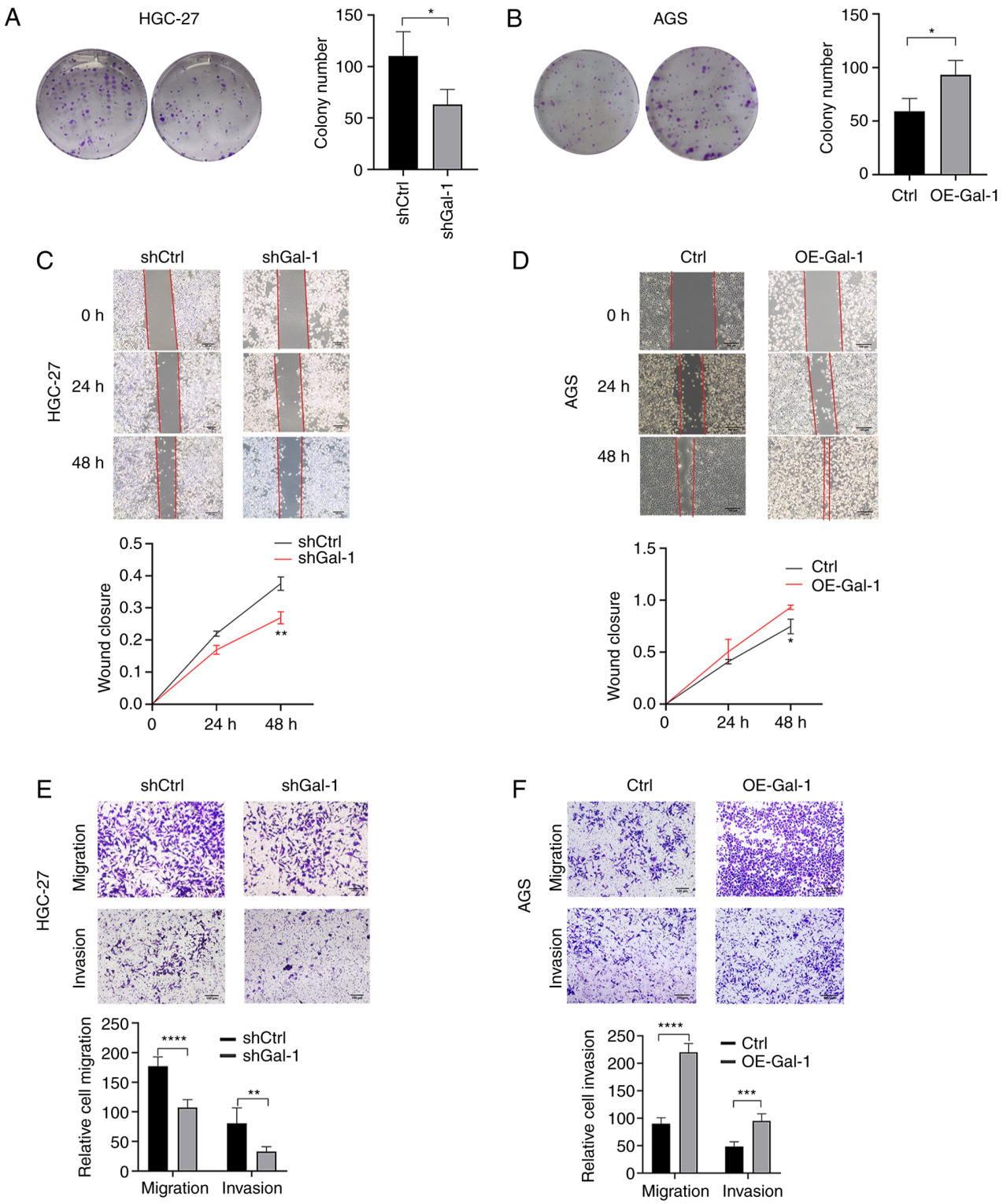

Figure 3. Gal-1 knockdown inhibits GC cell proliferation, migration and invasion, and Gal-1 OE promotes GC cell proliferation migration and invasion. (A and B) Detection of the proliferation of (A) HGC-27 cells after Gal-1 knockdown and (B) AGS cells after Gal-1 OE by colony formation assays. (C and D) Detection of the migration of (C) HGC-27 cells after Gal-1 knockdown and (D) AGS cells after Gal-1 OE by wound healing assay. (E and F) Detection of the migration and invasion of (E) HGC-27 cells after Gal-1 knockdown and (F) AGS cells after OE by Transwell assays. *P<0.05, **P<0.01, ***P<0.001 and ****P<0.0001. Gal-1, galectin-1; GC, gastric cancer; sh-, short hairpin; OE, overexpression.

and wound healing assays both showed that decreasing Gal-1 significantly reduced cell migration in the HGC-27 cell line (Fig. 3C and E). In addition, the Matrigel invasion experiments showed that blocking Gal-1 significantly reduced the ability to invade (Fig. 3E). The overexpression of Gal-1 in the AGS cell line, on the other hand, had the opposite impact of Gal-1 knockdown, as observed in Fig. 2E, leading to an increase in tumor cell proliferation, migration and invasion when compared with the control group (Fig. 3B, D and F; P<0.05).

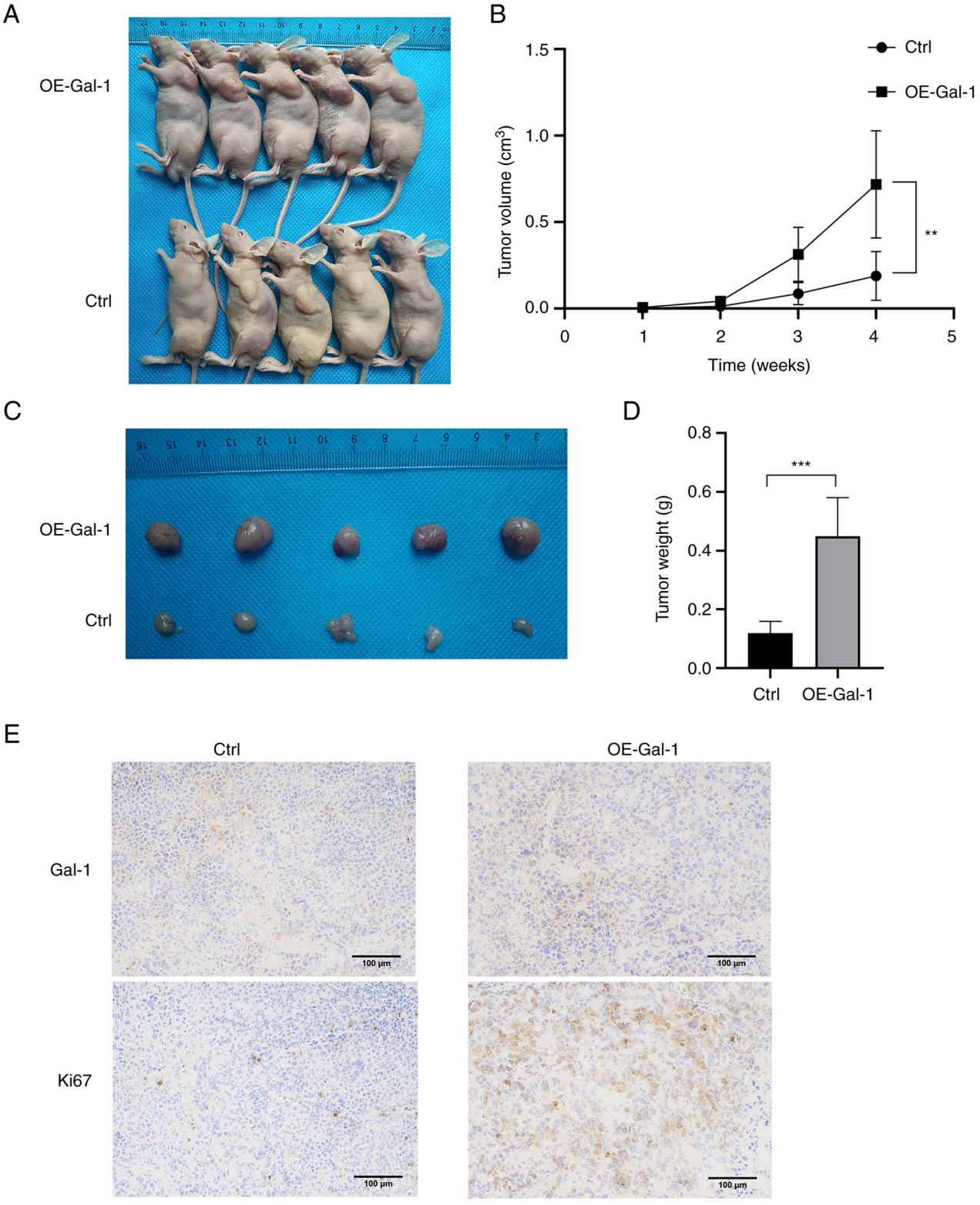

Figure 4. Effects of OE of Gal-1 on tumorigenesis in nude mice *in vivo*. (A) Xenograft models in nude mice were generated using AGS cells transfected with Ctrl (n=5) or Gal-1 lentiviral OE vector (n=5). (B) Subcutaneous tumor growth curve in nude mice. (C) Subcutaneous tumor images. (D) Detection of the tumor weight of AGS cells transfected with Gal-1 lentiviral OE vector after euthanasia. (E) Immunohistochemical detection of Gal-1 and Ki67 in xenograft tumors formed by AGS. **P<0.01 and ***P<0.001. OE, overexpression; Gal-1, galectin-1.

Overexpression of Gal-1 promotes the growth of tumors in nude mice. The xenograft tumor model was used to further explore the role of Gal-1 *in vivo*. Nude mice were injected with AGS cells that had been stably transfected with either the Ctrl or the OE-Gal-1 lentivirus, and the xenograft tumor growth was observed every week after the tumor injection. When compared with the Ctrl group, overexpression of Gal-1 almost caused the tumor to expand (Fig. 4A and B). The most significant tumor volume was 1.183 cm^3 in the OE-Gal-1 group and 0.384 cm^3 in the Ctrl group when

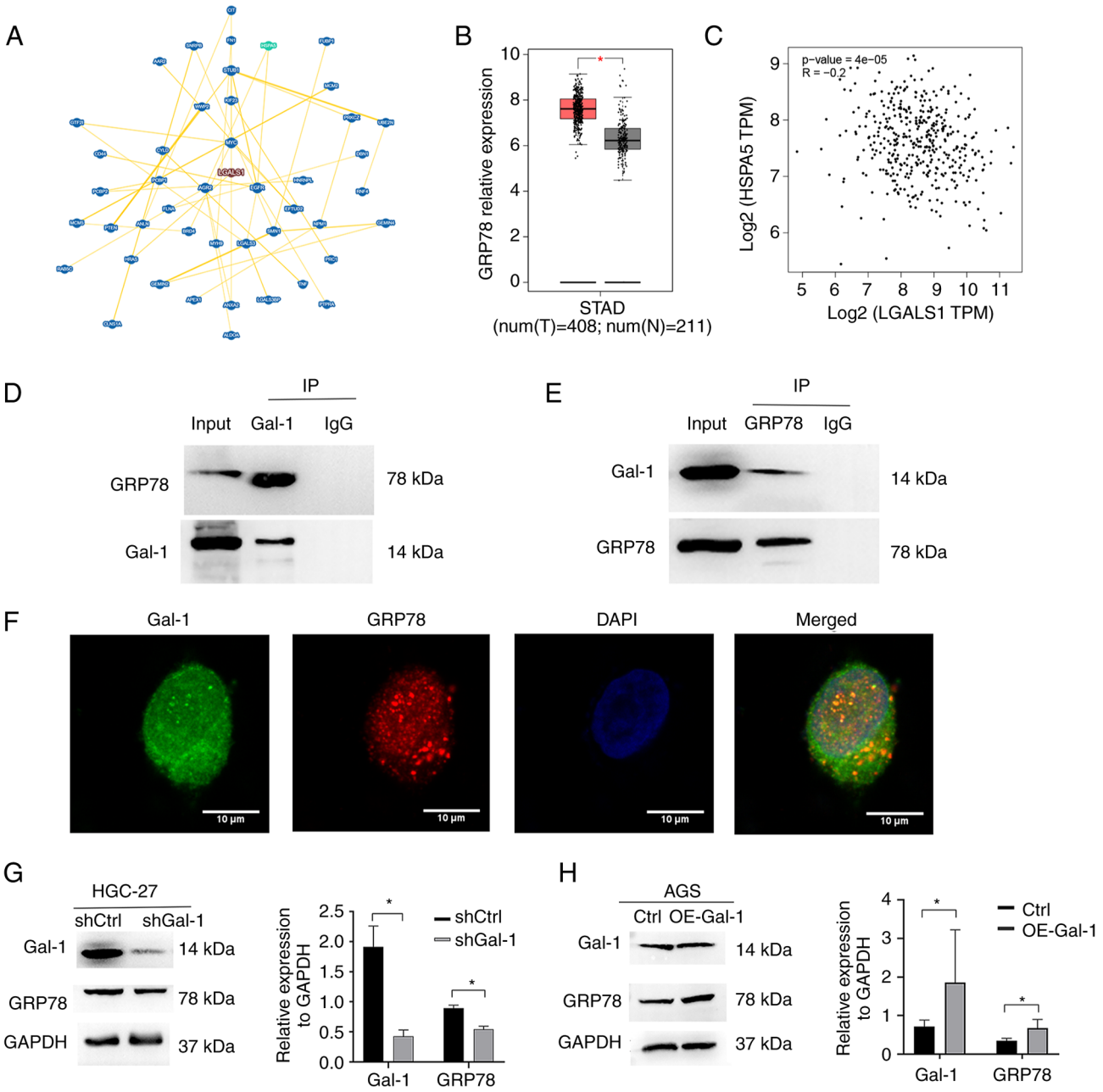

Figure 5. GRP78 is associated with Gal-1. (A) The interaction protein network of Gal-1 was revealed by the BioGRID database (https://thebiogrid.org/). (B) GRP78 mRNA expression in GC (n=408) and average (n=211) samples were evaluated using the online tool GEPIA. (C) The expression level of Gal-1 mRNA is independent of GRP78 mRNA in The Cancer Genome Atlas database. (D and E) Gal-1 physically interacted with GRP78. The endogenous proteins from HGC-27 cells were immunoprecipitated with IgG or antibodies against Gal-1 and GRP78, followed by western blot analysis and cell lysis for input. (F) Immunofluorescence colocalization of Gal-1 and GRP78 in GC cells (scale bar, 10 μm). (G) A western blot assay was performed to detect the GRP78 protein levels in the HGC-27 cells, knocking-down Gal-1. (H) Western blot analysis was performed to detect the GRP78 protein levels in the AGS cells overexpressing Gal-1. *P<0.05. GRP78, glucose-regulated protein 78; Gal-1, galectin-1; GC, gastric cancer; sh-, short hairpin; OE, overexpression.

the mice were euthanized four weeks later (Fig. 4C). The two groups of tumors were then weighed. Compared with the Ctrl group, the average weight of the OE-Gal-1 group was significantly larger (0.450±0.130 g vs. 0.120±0.039 g; P<0.05) (Fig. 4D). According to IHC examination, transfection with the lentiviral overexpression vector may successfully increase the level of Gal-1 expression in tumor tissues (Fig. 4E). After that, Ki-67 staining was employed to determine the capacity of tumors for proliferation. The findings demonstrated that tumor proliferative capacity was boosted by Gal-1 overexpression (Fig. 4E). The results demonstrated that overexpression of Gal-1 promoted GC xenograft tumor growth *in vivo*.

GRP78 oncoprotein is identified as a Gal-1-binding partner. The interacting proteins of Gal-1 were examined using the BioGRID database (https://thebiogrid.org/) in order to understand in an improved way the fundamental molecular mechanisms behind the tumor-promoting activity of Gal-1 in GC. According to the BioGRID database, Gal-1 is linked to 296 different proteins. A total of 45 proteins were ultimately identified as interacting with Gal-1 by high throughput and

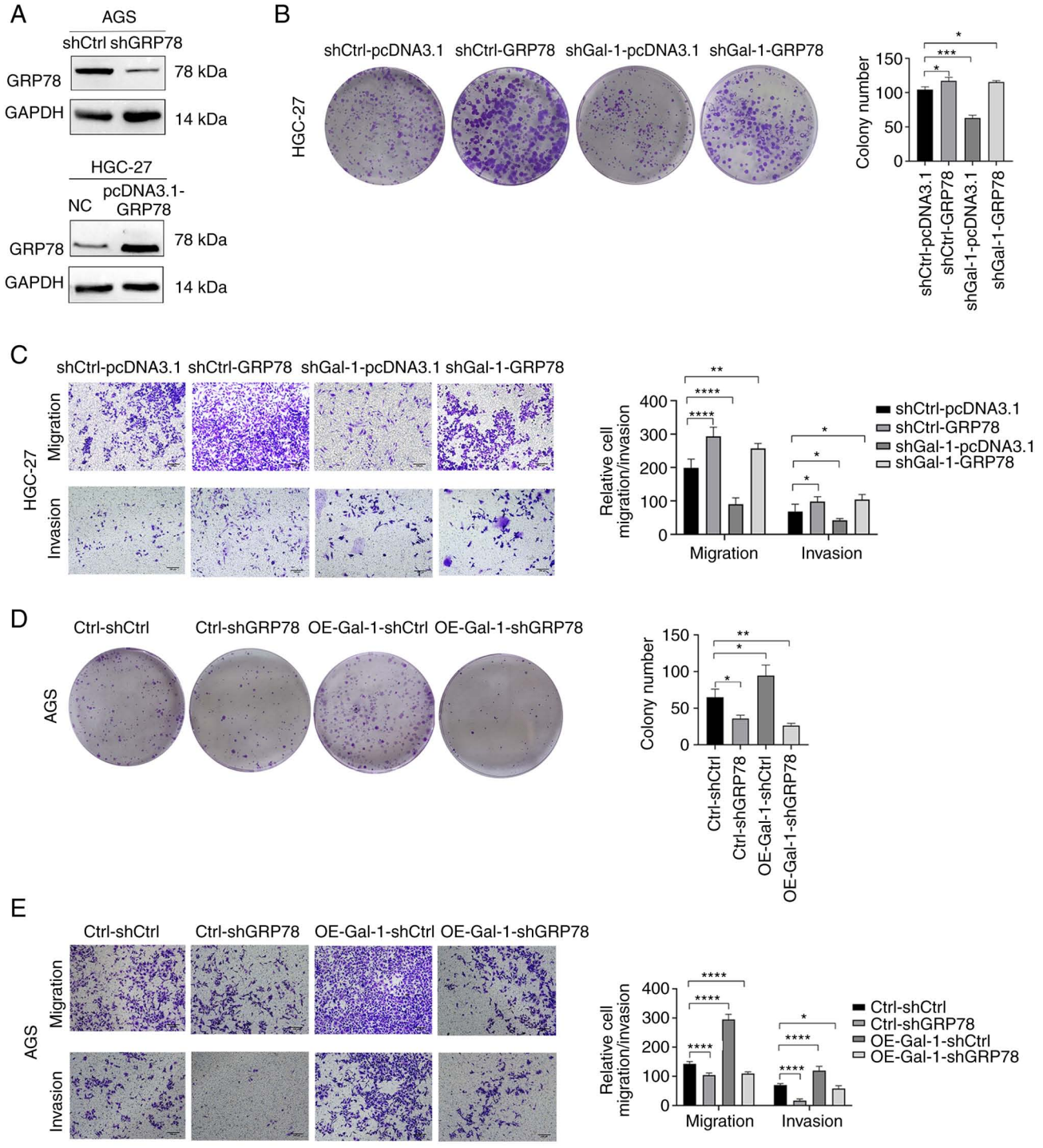

Figure 6. Tumor-promoting effect of Gal-1 is dependent on the upregulation of GRP78. (A) The knockdown and overexpression efficiency of GRP78 in AGS and HGC-27 cells was confirmed by western blot analysis. (B) Colony formation assay revealed that ectopic GRP78 expression restored the number of cell colonies in shGal-1HGC-27 cells. (C) Ectopic GRP78 expression promoted migration and invasion in shGal-1 HGC-27 cells. (D) Colony formation assay showed that lentivirus-mediated knockdown of GRP78, and ectopic Gal-1 expression inhibited cell growth of AGS cells. (E) Knockout GRP78 inhibited migration and invasion in OE-Gal-1 AGS cells. *P<0.05, **P<0.01, ***P<0.001 and ****P<0.0001. Gal-1, galectin-1; GRP78, glucose-regulated protein 78; sh-, short hairpin; OE, overexpression.

physical interactions after the search area was restricted and the minimum 3 evidence was chosen (Fig. 5A). Following validation, the heat shock protein GRP78, which is mostly localized at the ER and is encoded by HSPA5, was chosen for more examination. It is well recognized that GRP78 is involved in the migratory, invasion, angiogenesis and immune evasion processes that contribute to the advancement of GC (27-29). The mRNA expression of GRP78, similar to that of Gal-1, was significantly overexpressed in the TCGA GC cohort (Fig. 5B). In the TCGA GC cohort, there was also no discernible relationship between the genes for Gal-1 and GRP78 (Fig. 5C). Therefore, the present study concentrated on the interaction between the GRP78 and Gal-1 proteins. First, the function of the ER in HGC-27 cells cultivated in our lab was examined

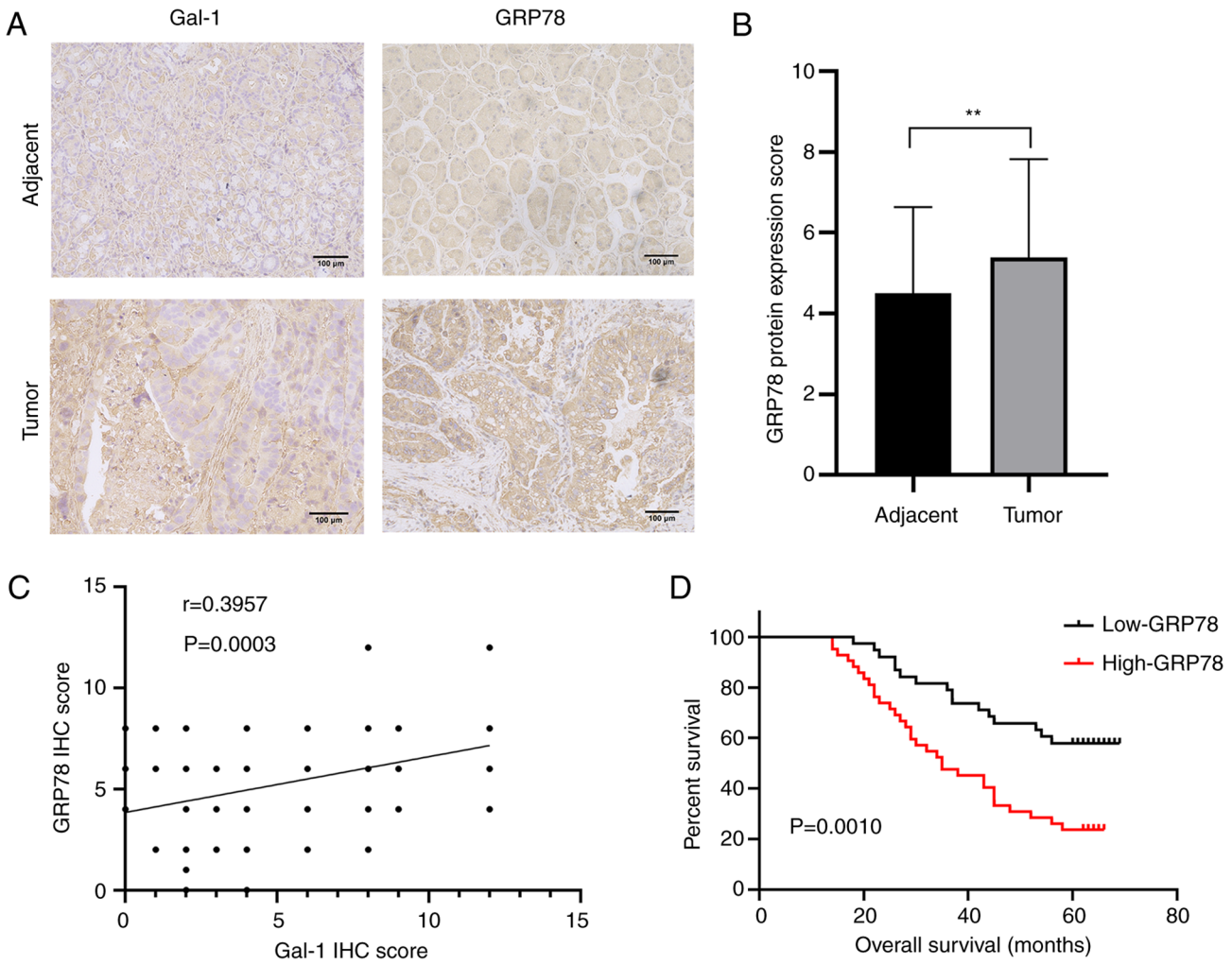

Figure 7. (A) The IHC assay of Gal-1 and GRP78 expression in GC tissues and corresponding adjacent normal tissues was performed, and the representative images were shown. (B) Qualification of GRP78 staining in TMAs described in panel A. The graph depicts the total score, the multiplication product of staining intensity and the percentage of stained cells. (C) Statistical analysis of the relationship between the expression level of GRP78 and Gal-1 (P-value: Spearman's correlation coefficient). (D) Kaplan-Meier overall survival curves for all 80 patients with GC stratified by high and low expression of GRP78. **P<0.01. Gal-1, galectin-1; GRP78, glucose-regulated protein 78; IHC, immunohistochemical; GC, gastric cancer.

using western blotting and immunofluorescence staining assays. As expected, the level of GRP78, the marker for ERS, was increased markedly after treated with Tunicamycin (ERS inducer, 2 μg/ml) for 24 h (29), (Fig. S1). Subsequently, by using a reciprocal Co-IP experiment, it was examined whether endogenous GRP78 and Gal-1 had a functional connection that increased GC development by controlling GRP78. AminoLink Plus Coupling Resin was used to immunoprecipitate the Gal-1 protein complex, and anti-Gal-1 or anti-GRP78 antibodies were used for the immunoblot. An anti-Gal-1-specific antibody easily identified a positive GRP78 signal in the Co-IP complex that was brought down (Fig. 5D). Gal-1 was also observed in the immunoprecipitated material that the anti-GRP78 antibody was able to draw down (Fig. 5E). In order to ascertain whether GRP78 had the same subcellular location as Gal-1, an immunofluorescence staining test was carried out. HGC-27 cells underwent dual immunostaining for GRP78 and Gal-1 to look for subcellular localization (Fig. 5F). In HGC-27 cells, GRP78 was largely expressed in the cytoplasm and nucleus, where Gal-1 is also found. Recombinant lentiviruses were employed to over- and under-express Gal-1 in AGS and HGC-27 cells in order to examine if Gal-1 affects GRP78 expression and activity. In the Lv-shGal-1 group (HGC-27), it was revealed that the expression of GRP78 was significantly downregulated compared with the control group (Fig. 5G). Additionally, it was identified that AGS cells with high levels of Gal-1 over-expressed GRP78 protein (Fig. 5H). This information taken together suggested a connection between GRP78 and Gal-1.

Gal-1 influences GC proliferation, invasion and migration through GRP78. To determine if GRP78 is essential for Gal-1-mediated GC development, a functional rescue test was carried out. First, western blotting verified the effectiveness of GRP78 overexpression and knockdown in AGS and HGC-27 cells (Fig. 6A). The next step was to co-transfection of HGC-27 cells with shGal-1 lentivirus and pcDNA 3.1-GRP78. The colony formation experiment revealed that ectopic GRP78 expression restored the ability of Gal-1 knockdown cells (shGal-1-pcDNA 3.1 group) to form colonies to baseline levels in HGC27 cells (Fig. 6B). Data from cell migration and invasion studies further showed that cells co-transfected with pcDNA 3.1-GRP78 had a limited ability to block cell migration and invasion by

Table III. Expression of GRP78 in gastric cancer with different clinicopathological variables using our own cohort.

Histopathological parameters	Total number (80)	Expression level of GRP78		P-value
		Low	High	
Age, years				
<65	33	17	16	0.547
≥65	47	21	26	
Sex				0.917
Male	51	24	27	
Female	29	14	15	
Tumor size				0.796
<6	43	21	22	
≥6	37	17	20	
Lauren type				0.184
Intestinal type	73	33	40	
Diffuse type	7	5	2	
Depth of invasion				0.049
T1, T2	29	18	11	
T3, T4	51	20	31	
Lymphonodus metastasis				0.025
N0, N1	40	24	16	
N2, N3	40	14	26	
Distant metastases				0.084
Negative	58	31	27	
Positive	22	7	15	
TNM stage				0.048
I-II	35	21	14	
III-IV	45	17	28	
Degree of differentiation				0.004
Highly	43	14	29	
Moderately and poorly	37	24	13	
Histological grade				0.506
I	8	5	3	
II	38	19	19	
III	34	14	20	
Venous invasion				
No	45	23	22	0.463
Yes	35	15	20	
Nerve invasion				0.284
No	35	19	16	
Yes	45	19	26	

GRP78, glucose-regulated protein 78.

shGal-1 (Fig. 6C). When OE-Gal-1 AGS cell proliferation, migration, and invasion were compared with an empty vector control, GRP78 knockdown significantly reduced all three (Fig. 6D and E). These results supported the hypothesis that the Gal-1/GRP78 axis controls the course of GC by mediating the action of Gal-1 tumor-promoting in GC. In addition, IHC was performed to clarify the connection between the levels of Gal-1 and GRP78 protein expression in 80 GC samples and matched non-tumor tissues. GRP78 protein levels were significantly greater in GC tissues than in matching para-cancerous tissues, according to results of GRP78 protein expression in 80 pairs of GC tumors and matched non-tumor tissues (Fig. 7A and B). Additionally, Gal-1 expression in GC tissues was significantly and favorably linked with GRP78 protein level expression

(R=0.3957, P<0.01; Fig. 7C). Additionally, the GRP78 expression in our sample group was measured and was found to be in contrast to the pathological characteristics in the dichotomized GRP78 status. According to the summary in Table III, GRP78 expression was positively connected with the degree of differentiation (P=0.004), lymphonodus metastasis (P=0.025), TNM stage (P=0.048) and depth of invasion (P=0.049). High GRP78 protein expression was found to be positively connected with poor OS in GC patients according to a Kaplan-Meier analysis (P=0.0010; Fig. 7D). GRP78 expression was strongly associated with the overall five-year survival rate in both univariate and multivariate analyses (Table II, P<0.05).

Discussion

Our earlier research (30,31) has extensively discussed the relationship between Gal-1 expression and GC in the present study. The analysis of Gal-1 expression in GC using multiple experimental techniques and databases was carried out for the first time. The present findings revealed that Gal-1 plays a tumor-promoting role in GC and that it is upregulated and crucial for enhancing GC proliferation and invasion via its interaction with GRP78.

The current study used data from the Oncomine and GEPIA databases to observe Gal-1 expression profiling in GC. The findings demonstrated that samples from GC patients had significantly higher levels of Gal-1 mRNA. Gal-1 protein expression was also found in both malignant and non-cancerous tissues. In line with a previous study by the authors (30), it was showed that the expression of Gal-1 was higher in GC tissues than in nearby non-cancerous tissues in our database. The tumor size, depth of invasion, LN metastasis, distant metastasis, TNM stage and GRP78 expression were all associated with high levels of Gal-1 expression. Additionally, an association between increased Gal-1 expression and lower patient survival rates was identified. It was determined that high expression of Gal-1 may be used as a poor prognostic factor for GC by analyzing the link between higher expression of Gal-1 and poor survival rate in our cohort.

A number of studies have revealed that targeting Gal-1 is a promising therapeutic approach to slow the progression of cancer in addition to the diagnostic and prognostic utility of this protein (31-33). Gal-1 knockdown in GC cells was found to considerably impede the ability of HGC-27 cells to proliferate, migrate, and invade, according to the following *in vitro* investigations of the study. However, exogenous overexpression of Gal-1 facilitated AGS tumor cell motility, invasion and proliferation. Additional *in vivo* animal investigations revealed that, as compared with the Ctrl group, GC cells overexpressing Gal-1 grew larger in a nude mouse model of the disease. These findings indicated that Gal-1 promotes tumor growth in GC.

Gal-1 is widely expressed by various tissues, including natural killer cells and endothelial cells, and is encoded by the LGALS1 gene (34). Gal-1 has been implicated in a number of biological processes, including cell proliferation, differentiation, migration, invasion, apoptosis, homeostasis and vascular embryogenesis in a number of malignancies, according to previous studies (35-37). In other words, depending on the kind of cell and the context of the cell, Gal-1 can bind and cross-link glycoconjugates on the cell surfaces or ECM and regulate a variety of biological processes, including immunosuppression, angiogenesis and metastasis. Additionally, it has been established through IHC that initial tumor sections have significant levels of Gal-1 expression throughout (38-40). Gao *et al* (41) revealed that Gal-1 was overexpressed in breast cancer and hypothesized that the interaction between the N-terminus of Gal-1 and the FKH domain of FOXP3 prevented FOXP3 from having tumor-suppressive effects.

On the other hand, Gal-1 can bind to substances that boost their ability to promote carcinogenesis and metastasis in carcinoma. Gal-1 was assessed in hepatocellular carcinoma (HCC) tissues, according to Leung *et al* (42); the amount of serum Gal-1 is associated with HBV and liver cirrhosis. Gal-1 additionally increases HCC cell motility, proliferation and growth through the overexpression of RER1. It was also showed that the combination of sorafenib and the particular Gal-1 inhibitor OTX008 inhibits tumor growth in an animal model in a synergistic manner. A recent study revealed that the HGSC-secreted factor cathepsin L triggered Gal-1 secretion autocrine, which enhances angiogenesis, proliferation and migration in the omental microvascular endothelial cell metastasis of HGSC via activating the ERK1/2 pathway (43). Kucińska *et al* (44) revealed that extracellular Gal-1 and Gal-3 interact directly with the sugar residues on fibroblast growth factor receptor 1 (FGFR1), inducing phosphorylation of FGFR1 and initiating downstream kinase ERK1/2 and PLCγ signaling pathway, which results in cell proliferation and avoidance of apoptosis.

In the present study, GRP78 was identified as a potential interaction partner in Gal-1-mediated tumor progression utilizing the BioGRID database and Co-IP analysis to clarify the mechanism by which Gal-1 drives GC formation. GRP78 is linked to a number of processes that contribute to the growth of cancer, including cell growth, angiogenesis, apoptosis, chemoresistance, cell survival and metabolism (13). Additionally, GRP78 was overexpressed on the plasma membrane of several cancers, including endometrial, hepatocellular, prostate and breast cancer. In a different biological setting, GRP78 proteins could have a dual role as oncogenes or tumour suppressors. By reducing the activity of the VEGF/VEGFR2 pathway, for instance, the inhibition of GRP78 reduced the growth of colon cancer (45). High surface expression of GRP78 decreased colon cancer tumor growth and proliferation while increasing the potential to invade due to higher levels of NRF-2 and heme oxygenase-1 expression (HO1) (46).

On the contrary, Yuan *et al* (47) showed that the overexpression of GRP78 caused an enhancement of proliferation, invasion and migration and increased the percentage of cells in the S phase of the cell cycle due to a rise in matrix metalloproteinase-2 and 9 (MMP-2 and MMP-9) secretion level. It was revealed that GRP78 could be physically interacting with IGF1-R and redistributed from the ER to the surface of hepatoma cells by IGF-I, promoting cellular proliferation, migration and invasion activity (48). Several studies reported that various ligands could interact with GRP78, eliciting diverse signaling responses. Qian *et al* (49) showed that SCNN1B exhibited post-tumor-suppressive function through ubiquitination-dependent degradation of GRP78 by regulating the UPR signaling pathway. In a previous study, it was identified that

the interaction between GRP78 and a2-macroglobulin (a2M) increased prostate cancer cell survival and migration/invasion via activating the PAK-2/MAPK and PI3K pathways, in which GRP78 functioned as an a2M receptor (50). The aberrant expression of GRP78 in GC is explained in the current study by a unique mechanism. It was revealed that GRP78 interacts with Gal-1 using bioinformatic techniques and Co-IP tests. The co-localization of Gal-1 and GRP78 in the cytoplasm and nucleus was revealed by immunofluorescence labeling.

Furthermore, it was demonstrated that ectopic production of Gal-1 in AGS cells had the opposite effect on the expression of GRP78 from knocking down Gal-1 in HGC-27 cells, which reduced the expression of GRP78. As previously indicated, increased expression of GRP78 encourages the growth, invasion, and migration of tumors. As a result, it was suggested that GRP78 may play a crucial part in the progression of GC caused by Gal-1. Furthermore, ectopic GRP78 expression significantly increased the proliferation, migration and invasion of Gal-1 knockdown GC cell line, according to function rescue assays. The function of Gal-1 overexpression was consistently hampered by silencing GRP78. These findings demonstrated the critical part GRP78 plays in tumor growth caused by Gal-1. Notably, this GRP78 rescue function was insufficient, suggesting that Gal-1 may potentially advance GC through additional targets. According to previous studies (42-44), it was hypothesized that Gal-1 that is upregulated promotes the production of the GRP78 protein, transports it from the ER to the nucleus, and anchors. Nevertheless, more information about the precise mechanism has to be provided.

It was identified that the expression of GRP78 was upregulated in GC in our clinical sample sequence. Additionally, the degree of differentiation, lymphonodus metastasis, TNM stage and depth of invasion were statistically linked with the expression, which was consistent with previous results (21). In GC samples, GRP78 and Gal-1 expression levels are strongly associated, and patients with high GRP78 expression had a bad prognosis.

There were a number of limitations to the present study. First, track of OS of patients was just kept; we did not track their survival free from disease. Second, more samples should be included in the present investigation. The inability to identify the precise chemical mechanism by which Gal-1 interacts with GRP78 to advance GC along the cellular signaling pathway is another drawback.

In conclusion, it was determined that the protein Gal-1 plays a crucial role in mediating migration, invasion and proliferation. The connection between Gal-1 and GRP78, which results in the proliferation, invasion and migration of GC cells, is now understood in an improved way thanks to the present study. The present research may lead to the identification of new therapeutic targets for the Gal-1 and GRP78 pathways for the treatment of GC and may also provide guidance for existing targets.

Acknowledgements

The authors would like to thank Professor Liu-Hua Wang (Yangzhou Key Laboratory of Basic and Clinical Transformation of Digestive and Metabolic Diseases, Yangzhou, Jiangsu 225001, P.R. China) for providing technical support.

Funding

The present study was supported by the National Natural Science Foundation of China (grant no. 81972269).

Availability of data and materials

The datasets used and/or analyzed during the current study are available from the corresponding author on reasonable request.

Authors' contributions

QZ, D-RW and MA conceived the study. YW, DT and WW provided methodology. Q-NS, C-YZ, H-HZ and X-DZ conducted experimental investigation. C-YZ provided resources. QZ, DT and WW prepared and wrote the original draft. H-HZ and D-RW acquired funding. QZ and D-RW confirm the authenticity of all the raw data. All authors read and approved the final manuscript.

Ethics approval and consent to participate

The studies involving human participants were reviewed and approved (approval no. 2019KY-022) by the Ethics Committee of the Northern Jiangsu People's hospital, the Clinical Medical School, Yangzhou University Ethics Committee (Yangzhou, China). Written informed consent was obtained from all participants. The animal study was reviewed and approved (approval no. 202111020) by the Ethics Committee of Yangzhou University (Yangzhou, China).

Patient consent for publication

Not applicable.

Competing interests

The authors declare that they have no competing interests.

References

1. Machlowska J, Baj J, Sitarz M, Maciejewski R and Sitarz R: Gastric cancer: Epidemiology, risk factors, classification, genomic characteristics and treatment strategies. Int J Mol Sci 21: 4012, 2020.
2. Wong MCS, Huang J, Chan PSF, Choi P, Lao XQ, Chan SM, Teoh A and Liang P: Global incidence and mortality of gastric cancer, 1980-2018. JAMA Netw Open 4: e2118457, 2021.
3. Joshi SS and Badgwell BD: Current treatment and recent progress in gastric cancer. CA Cancer J Clin 71: 264-279, 2021.
4. Camby I, Le Mercier M, Lefranc F and Kiss R: Galectin-1: A small protein with major functions. Glycobiology 16: 137R-157R, 2006.
5. Carlini MJ, Roitman P, Nuñez M, Pallotta MG, Boggio G, Smith D, Salatino M, Joffé ED, Rabinovich GA and Puricelli LI: Clinical relevance of galectin-1 expression in non-small cell lung cancer patients. Lung Cancer 84: 73-78, 2014.
6. Huang CS, Tang SJ, Chung LY, Yu CP, Ho JY, Cha TL, Hsieh CC, Wang HH, Sun GH and Sun KH: Galectin-1 upregulates CXCR4 to promote tumor progression and poor outcome in kidney cancer. J Am Soc Nephrol 25: 1486-1495, 2014.
7. Zhang PF, Li KS, Shen YH, Gao PT, Dong ZR, Cai JB, Zhang C, Huang XY, Tian MX, Hu ZQ, *et al*: Galectin-1 induces hepatocellular carcinoma EMT and sorafenib resistance by activating FAK/PI3K/AKT signaling. Cell Death Dis 7: e2201, 2016.

8. Schulz H, Schmoeckel E, Kuhn C, Hofmann S, Mayr D, Mahner S and Jeschke U: Galectins-1, -3, and -7 are prognostic markers for survival of ovarian cancer patients. Int J Mol Sci 18: 1230, 2017.
9. Elola MT, Wolfenstein-Todel C, Troncoso MF, Vasta GR and Rabinovich GA: Galectins: Matricellular glycan-binding proteins linking cell adhesion, migration, and survival. Cell Mol Life Sci 64: 1679-1700, 2007.
10. Boyce M and Yuan J: Cellular response to endoplasmic reticulum stress: A matter of life or death. Cell Death Differ 13: 363-373, 2006.
11. Hetz C: The unfolded protein response: Controlling cell fate decisions under ER stress and beyond. Nat Rev Mol Cell Biol 13: 89-102, 2012.
12. Luo B and Lee AS: The critical roles of endoplasmic reticulum chaperones and unfolded protein response in tumorigenesis and anticancer therapies. Oncogene 32: 805-818, 2013.
13. Ibrahim IM, Abdelmalek DH and Elfiky AA: GRP78: A cell's response to stress. Life Sci 226: 156-163, 2019.
14. Cook KL, Soto-Pantoja DR, Clarke PA, Cruz MI, Zwart A, Wärri A, Hilakivi-Clarke L, Roberts DD and Clarke R: Endoplasmic reticulum stress protein GRP78 modulates lipid metabolism to control drug sensitivity and antitumor immunity in breast cancer. Cancer Res 76: 5657-5670, 2016.
15. Serrano-Negrón JE, Zhang Z, Rivera-Ruiz AP, Banerjee A, Romero-Nutz EC, Sánchez-Torres N, Baksi K and Banerjee DK: Tunicamycin-induced ER stress in breast cancer cells neither expresses GRP78 on the surface nor secretes it into the media. Glycobiology 29: 599, 2019.
16. Ahmadi A, Khansarinejad B, Hosseinkhani S, Ghanei M and Mowla SJ: miR-199a-5p and miR-495 target GRP78 within UPR pathway of lung cancer. Gene 620: 15-22, 2017.
17. Zhao G, Kang J, Xu G, Wei J, Wang X, Jing X, Zhang L, Yang A, Wang K, Wang J, *et al*: Tunicamycin promotes metastasis through upregulating endoplasmic reticulum stress induced GRP78 expression in thyroid carcinoma. Cell Biosci 10: 115, 2020.
18. Chern YJ, Wong JCT, Cheng GSW, Yu A, Yin Y, Schaeffer DF, Kennecke HF, Morin G and Tai IT: The interaction between SPARC and GRP78 interferes with ER stress signaling and potentiates apoptosis via PERK/eIF2α and IRE1α/XBP-1 in colorectal cancer. Cell Death Dis 10: 504, 2019.
19. Luo C, Xiong H, Chen L, Liu X, Zou S, Guan J and Wang K: GRP78 promotes hepatocellular carcinoma proliferation by increasing FAT10 expression through the NF-κB pathway. Exp Cell Res 365: 1-11, 2018.
20. Zhang X, Zhang Y, Lin F, Shi X, Xiang L and Li L: Shh overexpression is correlated with GRP78 and AR expression in primary prostate cancer: Clinicopathological features and outcomes in a Chinese cohort. Cancer Manag Res 12: 1569-1578, 2020.
21. Ogawa H, Kaira K, Takahashi K, Shimizu A, Altan B, Yoshinari D, Asao T and Oyama T: Prognostic role of BiP/GRP78 expression as ER stress in patients with gastric adenocarcinoma. Cancer Biomark 20: 273-281, 2017.
22. Tang Z, Li C, Kang B, Gao G, Li C and Zhang Z: GEPIA: A web server for cancer and normal gene expression profiling and interactive analyses. Nucleic Acids Res 45 (W1): W98-W102, 2017.
23. Rhodes DR, Yu J, Shanker K, Deshpande N, Varambally R, Ghosh D, Barrette T, Pandey A and Chinnaiyan AM: ONCOMINE: A cancer microarray database and integrated data-mining platform. Neoplasia 6: 1-6, 2004.
24. Oughtred R, Rust J, Chang C, Breitkreutz BJ, Stark C, Willems A, Boucher L, Leung G, Kolas N, Zhang F, *et al*: The BioGRID database: A comprehensive biomedical resource of curated protein, genetic, and chemical interactions. Protein Sci 30: 187-200, 2021.
25. Livak KJ and Schmittgen TD: Analysis of relative gene expression data using real-time quantitative PCR and the 2(-Delta Delta C(T)) method. Methods 25: 402-408, 2001.
26. MacArthur Clark JA and Sun D: Guidelines for the ethical review of laboratory animal welfare People's Republic of China national standard GB/T 35892-2018 [Issued 6 February 2018 effective from 1 September 2018]. Animal Model Exp Med 3: 103-113, 2020.
27. Fang S, Hong H, Li L, He D, Xu Z, Zuo S, Han J, Wu Q, Dai Z, Cai W, *et al*: Plasminogen kringle 5 suppresses gastric cancer via regulating HIF-1α and GRP78. Cell Death Dis 8: e3144, 2017.
28. Fu Z, Wang X, Zhou H, Li Y, Chen Y, Wang Z and Liu L: GRP78 positively regulates estrogen-stimulated cell growth mediated by ER-α36 in gastric cancer cells. Mol Med Rep 16: 8329-8334, 2017.
29. Kong Q, Zhang Z and Liang Z: Upregulating miR-637 aggravates endoplasmic reticulum stress-induced apoptosis in gastric cancer cells by suppressing calreticulin. Anim Cells Syst (Seoul) 24: 267-274, 2020.
30. You X, Wang Y, Wu J, Liu Q, Chen D, Tang D and Wang D: Prognostic significance of galectin-1 and vasculogenic mimicry in patients with gastric cancer. Onco Targets Ther 11: 3237-3244, 2018.
31. You X, Wu J, Wang Y, Liu Q, Cheng Z, Zhao X, Liu G, Huang C, Dai J, Zhou Y, *et al*: Galectin-1 promotes vasculogenic mimicry in gastric adenocarcinoma via the Hedgehog/GLI signaling pathway. Aging (Albany NY) 12: 21837-21853, 2020.
32. Nambiar DK, Aguilera T, Cao H, Kwok S, Kong C, Bloomstein J, Wang Z, Rangan VS, Jiang D, von Eyben R, *et al*: Galectin-1-driven T cell exclusion in the tumor endothelium promotes immunotherapy resistance. J Clin Invest 129: 5553-5567, 2019.
33. He YS, Hu YQ, Xiang K, Chen Y, Feng YT, Yin KJ, Huang JX, Wang J, Wu ZD, Wang GH and Pan HF: Therapeutic potential of galectin-1 and galectin-3 in autoimmune diseases. Curr Pharm Des 28: 36-45, 2022.
34. Arciniegas E, Carrillo LM, Rojas H, Pineda J, Ramírez R, Reyes O, Chopite M and Rocheta A: Plump endothelial cells integrated into pre-existing venules contribute to the formation of 'mother' and 'daughter' vessels in pyogenic granuloma: Possible role of galectin-1, -3 and -8. Scars Burn Heal 7: 2059513120986687, 2021.
35. Camby I, Belot N, Lefranc F, Sadeghi N, de Launoit Y, Kaltner H, Musette S, Darro F, Danguy A, Salmon I, *et al*: Galectin-1 modulates human glioblastoma cell migration into the brain through modifications to the actin cytoskeleton and levels of expression of small GTPases. J Neuropathol Exp Neurol 61: 585-596, 2002.
36. Kovács-Sólyom F, Blaskó A, Fajka-Boja R, Katona RL, Végh L, Novák J, Szebeni GJ, Krenács L, Uher F, Tubak V, *et al*: Mechanism of tumor cell-induced T-cell apoptosis mediated by galectin-1. Immunol Lett 127: 108-118, 2010.
37. Horiguchi N, Arimoto K, Mizutani A, Endo-Ichikawa Y, Nakada H and Taketani S: Galectin-1 induces cell adhesion to the extracellular matrix and apoptosis of non-adherent human colon cancer Colo201 cells. J Biochem 134: 869-874, 2003.
38. Kim HJ, Jeon HK, Cho YJ, Park YA, Choi JJ, Do IG, Song SY, Lee YY, Choi CH, Kim TJ, *et al*: High galectin-1 expression correlates with poor prognosis and is involved in epithelial ovarian cancer proliferation and invasion. Eur J Cancer 48: 1914-1921, 2012.
39. Saussez S, Cucu DR, Decaestecker C, Chevalier D, Kaltner H, André S, Wacreniez A, Toubeau G, Camby I, Gabius HJ and Kiss R: Galectin 7 (p53-induced gene 1): A new prognostic predictor of recurrence and survival in stage IV hypopharyngeal cancer. Ann Surg Oncol 13: 999-1009, 2006.
40. Chiang WF, Liu SY, Fang LY, Lin CN, Wu MH, Chen YC, Chen YL and Jin YT: Overexpression of galectin-1 at the tumor invasion front is associated with poor prognosis in early-stage oral squamous cell carcinoma. Oral Oncol 44: 325-334, 2008.
41. Gao Y, Li X, Shu Z, Zhang K, Xue X, Li W, Hao Q, Wang Z, Zhang W, Wang S, *et al*: Nuclear galectin-1-FOXP3 interaction dampens the tumor-suppressive properties of FOXP3 in breast cancer. Cell Death Dis 9: 416, 2018.
42. Leung Z, Ko FCF, Tey SK, Kwong EML, Mao X, Liu BHM, Ma APY, Fung YME, Che CM, Wong DKH, *et al*: Galectin-1 promotes hepatocellular carcinoma and the combined therapeutic effect of OTX008 galectin-1 inhibitor and sorafenib in tumor cells. J Exp Clin Cancer Res 38: 423, 2019.
43. Pranjol MZI, Zinovkin DA, Maskell ART, Stephens LJ, Achinovich SL, Los' DM, Nadyrov EA, Hannemann M, Gutowski NJ and Whatmore JL: Cathepsin L-induced galectin-1 may act as a proangiogenic factor in the metastasis of high-grade serous carcinoma. J Transl Med 17: 216, 2019.
44. Kucińska M, Porębska N, Lampart A, Latko M, Knapik A, Zakrzewska M, Otlewski J and Opaliński Ł: Differential regulation of fibroblast growth factor receptor 1 trafficking and function by extracellular galectins. Cell Commun Signal 17: 65, 2019.
45. Kuo LJ, Hung CS, Chen WY, Chang YJ and Wei PL: Glucose-regulated protein 78 silencing down-regulates vascular endothelial growth factor/vascular endothelial growth factor receptor 2 pathway to suppress human colon cancer tumor growth. J Surg Res 185: 264-272, 2013.

46. Chang YJ, Chen WY, Huang CY, Liu HH and Wei PL: Glucose-regulated protein 78 (GRP78) regulates colon cancer metastasis through EMT biomarkers and the NRF-2/HO-1 pathway. Tumour Biol 36: 1859-1869, 2015.
47. Yuan XP, Dong M, Li X and Zhou JP: GRP78 promotes the invasion of pancreatic cancer cells by FAK and JNK. Mol Cell Biochem 398: 55-62, 2015.
48. Yin Y, Chen C, Chen J, Zhan R, Zhang Q, Xu X, Li D and Li M: Cell surface GRP78 facilitates hepatoma cells proliferation and migration by activating IGF-IR. Cell Signal 35: 154-162, 2017.
49. Qian Y, Wong CC, Xu J, Chen H, Zhang Y, Kang W, Wang H, Zhang L, Li W, Chu ESH, *et al*: Sodium channel subunit SCNN1B suppresses gastric cancer growth and metastasis via GRP78 degradation. Cancer Res 77: 1968-1982, 2017.
50. Bastida-Ruiz D, Wuillemin C, Pederencino A, Yaron M, Martinez de Tejada B, Pizzo SV and Cohen M: Activated α_2-macroglobulin binding to cell surface GRP78 induces trophoblastic cell fusion. Sci Rep 10: 9666, 2020.